arXiv:1802.06856v2 [astro-ph.EP] 21 Feb 2018

Version: March 15, 2022

The Habitable Zone of Kepler-16: Impact of Binarity and Climate Models

S. Y. Moorman[1], B. L. Quarles[2], Zh. Wang[1], and M. Cuntz[1]

[1]*Department of Physics, Box 19059*

University of Texas at Arlington, Arlington, TX 76019;

sarah.moorman@mavs.uta.edu; zhaopeng.wang@mavs.uta.edu; cuntz@uta.edu

[2]*Homer L. Dodge Department of Physics and Astronomy*

University of Oklahoma, Norman, OK 73019;

billylquarles@gmail.com

ABSTRACT

We continue to investigate the binary system Kepler-16, consisting of a K-type main-sequence star, a red dwarf, and a circumbinary Saturnian planet. As part of our study, we describe the system's habitable zone based on different climate models. We also report on stability investigations for possible Earth-mass Trojans while expanding a previous study by B. L. Quarles and collaborators given in 2012. For the climate models we carefully consider the relevance of the system's parameters. Furthermore, we pursue new stability simulations for the Earth-mass objects starting along the orbit of Kepler-16b. The eccentricity distribution as obtained prefers values close to circular, whereas the inclination distribution remains flat. The stable solutions are distributed near the co-orbital Lagrangian points, thus enhancing the plausibility that Earth-mass Trojans might be able to exist in the Kepler-16(AB) system.

Subject headings: astrobiology — binaries: general — celestial mechanics — planetary systems — stars: individual (Kepler-16)

1. Introduction

Kepler-16 is a well-documented example of a closely separated binary system with a Saturnian planet in a P-type orbit (Slawson *et al.* 2011; Doyle *et al.* 2011). P-type orbit means that the planet encircles both stars instead of only one star with the other star acting as a perturber (Dvorak 1982). Previous results on the existence and orbital properties of planets in binary systems have been given by, e.g., Raghavan *et al.* (2006, 2010) and Roell *et al.* (2012), among others. Detailed information on the abundance of circumstellar planets has been given by Wang *et al.* (2014) and Armstrong *et al.* (2014). So far, eleven circumbinary planets have been discovered by *Kepler* with Kepler-453b and Kepler-1647b constituting number 10 and 11, as reported by Welsh *et al.* (2015) and Kostov *et al.* (2016), respectively.

The main purpose of the *Kepler* mission is to identify exoplanets via the transit method near or within the host star's habitable zone (HZ). The lion's share of stars-of-study encompass main-sequence stars of spectral types G, K, and M, with latter ones also referred to as red dwarfs. Recent catalogs of stars studied by *Kepler* have been given by Kirk *et al.* (2016) and Thompson *et al.* (2017). Here Thompson *et al.* (2017) offer the latest results for the general catalog from *Kepler*, as it contains all observed objects, including circumbinary planets, potentially habitable planets, and (most likely) non-habitable planets. On the other hand, the catalog by Kirk *et al.* (2016) is mostly focused on eclipsing binary systems.

Previous theoretical work about circumbinary planets in binary systems has been given by, e.g., Kane & Hinkel (2013), Eggl *et al.* (2013), Haghighipour & Kaltenegger (2013), Cuntz (2014, 2015), Zuluaga *et al.* (2016), Popp & Eggl (2017), Shevchenko (2017), and Wang & Cuntz (2017), and references therein. These types of studies focus on the formation, orbital stability, secular evolution, and/or environmental forcings pertaining to those systems. For example, recently, Wang & Cuntz (2017) presented fitting formulae for the quick determination of the existence of P-type HZs in binary systems. Objects hosted by P-type systems which might be potentially habitable could include exoplanets, exomoons, and exo-Trojans. For Kepler-16, the latter two kinds of objects have been discussed by Quarles et al. (2012), hereafter QMC12.

Kepler-16(AB) is a pivotal example of a planet-hosting binary; it is 61 parsecs (199 light years) from Earth (see Table 1); for more detailed information see Doyle *et al.* (2011), and references therein. The system consists of the primary star, Kepler-16A, a K-dwarf of about 0.69 $M_{\odot}$, and the secondary star, Kepler-16B, a red dwarf star. The circumbinary planet of that system is similar to Saturn in mass and density. Kepler-16b has a nearly circular orbit with an eccentricity of approximately 0.007 and a small deviation in orbital inclination to that of its host stars indicating that it may have formed within the same circumbinary disk

as the two stars. Although Kepler-16b proves to be an interesting exoplanet, it is considered to be cold, gaseous, and ultimately uninhabitable. However, previous work by QMC12 has focused on the possibility of both Earth-mass exomoons and Trojans, which if existing may be potentially habitable. Among other considerations, we intend to expand the work by QMC12 in this article.

The structure of our paper is as follows. In Section 2, we report the stellar parameters. A special effort is made to determine the effective temperature of Kepler-16B. Section 3 discusses the HZ of the Kepler-16(AB) binary system in consideration of different types of climate models available in the literature. For tutorial reasons, we also discuss the HZ of Kepler-16A, with Kepler-16B assumed absent. In Section 4, we consider the previous results by QMC12 for Earth-mass moons and Trojans in relationship to Kepler-16's HZ. Furthermore, additional stability simulations based on a modified version of the mercury6 integration package are pursued to explore the possible parameter space of stable objects in the Kepler-16(AB) system. Our summary and conclusions are given in Section 5.

2. Stellar Parameters

Regarding our study, stellar parameters are of pivotal importance for the calculation of stellar HZs as well as for orbital stability simulations of possible exomoons and Trojan objects. Most relevant parameters of the Kepler-16(AB) system have been previously reported by Doyle *et al.* (2011), as they announce a transiting circumbinary planet observed by the *Kepler* spacecraft. Kepler-16A was identified as a K-type main-sequence star with effective temperature, radius, and mass given as (see Table 1) 4450 ± 150 K, 0.6489 ± 0.0013 $R_{\odot}$, and 0.6897 ± 0.0035 $M_{\odot}$, respectively. Here the relative uncertainty bar is largest for the stellar effective temperature (see Table 2).

However, less information has been conveyed for Kepler-16B, which based on its mass of about 0.20255 $M_{\odot}$ (Doyle *et al.* 2011) is identified as a red dwarf. But Kepler-16B's effective temperature needs to be determined as well to compute the HZ for the Kepler-16 binary system. Thus, to determine Kepler-16B's stellar effective temperature, we utilize the mass – effective temperature relationship by Mann *et al.* (2013). They have analyzed moderate resolution spectra for a set of nearby K and M dwarfs with well-known parallaxes and interferometrically determined radii to define their effective temperatures, among other quantities. They also adopt state-of-the-art PHOENIX atmosphere models, as described. Thus, we conclude that the effective temperature of Kepler-16B is 3308 ± 110 K (see Fig. 1). Here the uncertainty bar has been estimated based on the results of similar objects included in the sample. From other work as, e.g., that by Kirkpatrick *et al.* (1991) and Baraffe *et al.*

(1998) the spectral type of Kepler-16B has been deduced as ∼M3 V. Both the effective temperature and radius of Kepler-16B are important for determining the different types of HZs of the Kepler-16(AB) system (see Sect. 4).

3. The Kepler-16 Habitable Zone

A crucial aspect of this study is the evaluation of Kepler-16's HZ. The HZ is a region around a star or a system of stars in which terrestrial planets could potentially have surface temperatures at which liquid water could exist, given a sufficiently dense atmosphere (e.g., Kasting *et al.* 1993; Jones *et al.* 2001; Underwood *et al.* 2003). When determining the HZ, both inner limits and outer limits are calculated, in response to different types of criteria, thus defining the HZ. The determination of the location of the HZ is significant in the context of theoretical studies as well as for the purpose of planet search missions (e.g., Lammer *et al.* 2009; Kasting *et al.* 2014; Kaltenegger 2017, and references therein).

Inner limits previously used for stellar HZs include those set by the recent Venus (RV), the runaway greenhouse effect, and the onset of water loss. Furthermore, outer limit of the stellar HZ has been set by the first CO_2 condensation, the maximum greenhouse effect for a cloud-free CO_2 atmosphere and the early Mars (EM) setting. For example, Kasting *et al.* (1993) describe the runaway greenhouse effect such that the greenhouse phenomenon is enhanced by water vapor, thus promoting surface warming. The latter further increases the atmospheric vapor content, thus resulting in an additional rise of the planet's surface temperature. Consequently, this will lead to the rapid evaporation of all surface water. On the other hand (see, e.g., Underwood *et al.* 2003), the water loss criterion means that an atmosphere is warm enough to have a wet stratosphere, from where water is gradually lost by atmospheric chemical processes to space.

Table 3 shows the HZ limits for Kepler-16A, treated as a single star, for tutorial reasons. Here GHZ denotes the general habitable zone, bracketed by the runaway greenhouse and maximum greenhouse criteria, whereas RVEM denotes the kind of HZ, defined by the settings of recent Venus and early Mars; this latter type of HZ is also sometimes referred to as (most) optimistic HZ; see, e.g., Kaltenegger (2017) and references therein. Figure 2 and Tables 3 and 4 convey the results for the various HZ limits as well as for the GHZ and RVEM. The most recent results based on Kopparapu *et al.* (2013, 2014) have been included as well, which indicate updated HZ limits. For the inner and outer HZ limits, they assumed H_2O and CO_2 dominated atmospheres, respectively, while scaling the background N_2 atmospheric pressure with the radius of the planet. Moreover, from said climate model, several equations were generated, which correspond to select inner and outer HZ limit criteria.

Surely, most of our study focuses on Kepler-16 as a binary thus taking into account both Kepler-16A (an orange dwarf) and Kepler-16B (a red dwarf); see Table 1 for data. The computation of the GHZ and RVEM of Kepler-16(AB) follows the work by Cuntz (2014, 2015) and Wang & Cuntz (2017). Information is given in Fig. 3; here RHZ refers to the so-called radiative habitable zone (applicable to both the GHZ and RVEM), which is based on the planetary climate enforcements set by both stellar components, while deliberately ignoring the orbital stability criterion regarding a possible system planet. Figure 3 indicates the inner and outer RHZ limits with the inner HZ limit defined as the maximum radial distance of the inner RHZ (red lines) and the outer HZ limit defined as the minimum radial distance of the outer RHZ (blue lines). This approach conveys the HZ region for GHZ (darkest green) and RVEM (medium green) criteria (see also Table 5). As expected the RVEM criteria produces a more generous HZ region. We also indicate the orbital stability limit (black dashed line) based on Holman & Wiegert (1999), referred to as $a_{\rm orb}$. In fact it is found that the widths of the GHZ and RVEM for Kepler-16(AB) are significantly less than for Kepler-16A (single star approach), owing to the additional criterion of orbital stability for possible system planets.

Previous work by Mischna *et al.* (2000) argues that the HZ about a main-sequence star might be further extended if CO_2 cloud coverage is assumed. In the case of the Sun, this assumption would amount to an outer limit of 2.40 AU for the hereupon defined extended habitable zone (EHZ)[1]. Von Bloh *et al.* (2007) have explored the habitability around Gliese 581 with focus on the possible planet GJ 581d. They argue that the RHZ could be further extended if the atmospheric structure is determined by particularly high base pressures. Thus, the outer limit for the EHZ is not very well constrained, but could be parameterized as $\epsilon\sqrt{L}$ with ϵ in the likely range between 2.0 and 3.0 and L defined as stellar luminosity (in units of solar luminosity). Hence, $\epsilon = 2.4$ corresponds to the value of Mischna *et al.* (2000). Results for the EHZ of Kepler-16(AB) are given in Figure 4 and Table 6.

Another aspect of study is that concerning the GHZ and RVEM, we also have explored the impact of the observational uncertainties of the stellar luminosities on inner and outer

[1]The previous work by Mischna *et al.* (2000) has been superseded by more recent studies, including those given by Halevy *et al.* (2009), Pierrehumbert & Gaidos (2011), Wordsworth *et al.* (2013), and Kitzmann (2016); see also summary by Seager (2013). For example, Kitzmann (2016) argued that the heating assumed by Mischna *et al.* (2000) has been overestimated, thus putting the extension of the outer HZ in question. However, in the following, we will parameterize the outer limit of Mischna *et al.* (2000), and the significance of our results will not rely on the full extent of the HZ introduced by them. Moreover, Pierrehumbert & Gaidos (2011) argued that planetary HZs could extend to up to 10 AU for single G-type stars (or, say, about 3 AU for single K-type stars, as indicated by their Fig. 1), which is well beyond the outer limit advocated by Mischna *et al.* (2000).

limits of the RHZs (see Figs. 5 and 6). It is found that the uncertainty in the stellar luminosity ΔL moves the inner and outer limits of both the GHZ and the RVEM by about $\pm 6\%$. Our results are summarized in Table 7. Here we also see that the inner limits of both the GHZ and RVEM are set by the additional criterion of orbital stability regarding possible circumbinary planets, referred to by Cuntz (2014) as PT habitability. Additionally, it is found that the HZ around Kepler-16A (if treated as a single star) would be significantly more extended than the HZ of Kepler-16(AB). Thus, Kepler-16B notably reduces the prospect of habitability in that system.

4. Stability Investigations for Earth-Mass Exomoons and Trojans

Previously, QMC12 have exemplary case studies for the orbital stability of Earth-mass objects (i.e., Trojan exoplanet or exomoon) in the Kepler-16(AB) system. Their numerical methods were based on the Wisdom-Holman mapping technique and the Gragg-Burlisch-Stoer algorithm (Grazier *et al.* 1996). The resulting equations of motion were integrated forward in time for 1 million years using a fixed/initial (WH/GBS) time step. QMC12 showed that, in principle, both Trojan exoplanets and exomoons are able to exist in the Kepler-16(AB) system. Figures 7 and 8 show the results by QMC12 together with the updated system's HZs, i.e., the GHZ, RVEM, and EHZ. It is found that the orbital settings of those objects are consistent with an EHZ (with $\epsilon \lesssim 2.2$) or with the RVEM if upper limits of the stellar luminosities, consistent with the observational uncertainties, are considered.

In order to better understand the dynamical domain of possible exo-Trojans, we perform additional 5,000 stability simulations using a modified version of the mercury6 integration package that is optimized for circumbinary systems (Chambers *et al.* 2002). In these simulations, we adopt the orbital parameters from Doyle *et al.* (2011) for the binary components and the Saturnian planet. We also consider Earth-mass objects with different initial conditions. Table 8 conveys the initial conditions for exomoon sample cases, which are: the semimajor axis a, eccentricity e, inclination i, argument of periastron ω, and mean anomaly M for each body. A simulation is terminated when the Earth-mass body either crosses the binary orbit or has a radial distance from the center of mass greater than 100 AU; this will be viewed as an ejection.

The orbital evolution of the four bodies are evaluated on a 10 Myr timescale. The initial orbital elements are chosen using uniform distributions. The initial semimajor axis of the Earth-mass object is selected from values ranging from 0.6875 AU to 0.7221 AU (i.e., $\pm$ 0.5 Hill radii); furthermore, eccentricities are limited to 0.1 and inclinations are limited to 1°. The initial argument of periastron and mean anomalies are selected randomly between 0°

and 360°. The statistical distributions of the surviving population are shown in Figure 9 to illustrate possible correlations between parameters.

Overall ∼10% of the simulations (496) are identified as stable (i.e., survived for 10 Myr) as depicted in Figure 10. By delineating the stable (cyan) and unstable (gray) points, it is seen that the stable initial conditions correspond to Trojans and are separated in relative phase from Kepler-16b by ∼60° to 90°. This also appears in Figure 9 through the distribution for λ^*, the relative mean longitude. The inclinations of the orbitally stable Earth-mass objects in Fig. 9 remain uniformly distributed and thus are unlikely to affect the overall stability. Figure 11 illustrates the orbital evolution in a rotated-reference frame of two initial conditions taken from Figure 10. The panels of Fig. 11 show the first ∼1,000 years of orbital evolution, where the run in the top panel would continue in a Trojan orbit for the 10 Myr simulation time and the other run (bottom panel) evolves in a horseshoe orbit, which quickly becomes unstable. We also found that the eccentricity distribution as obtained prefers values close to circular, whereas the relative mean longitude distribution reflects, by a factor of two, more trailing orbits than preceding orbits.

5. Summary and Conclusions

The purpose of our study is to continue investigating the habitable zone as well as the general possibility of Earth-mass exomoons and Trojans in Kepler-16. The binary system Kepler-16(AB) consists of a low-mass main-sequence star, a red dwarf and a circumbinary Saturnian planet. The temperatures of the two stellar components are given as 4450 ± 150 K and 3308 ± 110 K, respectively. Previously, QMC12 pursued an exploratory study about this system, indicating that based on orbital stability considerations both Earth-mass exomoons and Earth-mass Trojan planets might be possible. The aim of the present study is to offer a more thorough analysis of this system. We found the following results:

(1) As previously said by QMC12, Kepler-16 possesses a circumbinary HZ; its width depends on the adopted climate model. Customarily, these HZs are referred to as GHZ and RVEM; the latter is also sometimes referred to as optimistic HZ (e.g., Kopparapu *et al.* 2013; Kaltenegger 2017). For objects of thick CO_2 atmospheres including clouds, the HZ is assumed to be further extended, thus giving rise to the EHZ as proposed by Mischna *et al.* (2000).

(2) Our work confirms earlier simulations by QMC12 that both Earth-mass exomoons and Earth-mass Trojan planets could stably orbit in that system. However, in this study, we

adopted longer timescales and also explored the distributions of eccentricity and inclinations of the Earth-mass test objects considered in our study.

(3) Exomoons and Trojans, associated with the Saturnian planet, are found to be situated in the lower portion of the EHZ (i.e., $\epsilon \lesssim 2.2$). A more detailed analysis also implies that the distances of those objects may be consistent with the RVEM (i.e., optimistic HZ) if a relatively high luminosity for the stellar components is assumed (but still consistent with the uncertainty bars) or if the objects are allowed to temporarily leave the RVEM-HZ without losing habitability. The latter property is maintained if habitability is provided by a relatively thick atmosphere Williams & Pollard (2002).

(4) For tutorial reasons, we also compared the HZ of the system's primary to that of the binary system. We found that the latter is reduced by 42% (GHZ) and 48% (RVEM) despite the system's increase in total luminosity given by the M-dwarf. The reason is that for the binary, the RHZ is unbalanced and it is further reduced by the additional requirement of orbital stability as pointed out previously (e.g., Eggl *et al.* 2013; Cuntz 2014).

(5) Moreover, we pursued new stability simulations for Earth-mass objects while taking into account more general initial conditions. The attained eccentricity distribution prefers values close to circular, whereas the inclination distribution is relatively flat. The distribution in the initial relative phase indicates that the stable solutions are distributed near the co-orbital Lagrangian points, thus increasing the plausibility for the existence of those objects.

Our study shows that the binary system Kepler-16(AB) has a HZ of notable extent, though smaller than implied by the single-star approach, with its extent critically depending on the assumed climate model for the possible Earth-mass Trojan planet or exomoon. Thus, Kepler-16 should be considered a valuable target for future planetary search missions. Moreover, it is understood that comprehensive studies of habitability should take into account additional forcings by planet host stars, such as stellar activity and strong winds expected to impact planetary conditions as indicated through analyses by, e.g., Lammer (2007), Tarter *et al.* (2007), Lammer *et al.* (2009), Kasting *et al.* (2014), and Kaltenegger (2017). Recent articles about the impact on stellar activity on prebiotic environmental conditions have been given by, e.g., Cuntz & Guinan (2016) and Airapetian *et al.* (2017).

This work has been supported by the Department of Physics, University of Texas at Arlington (UTA). The simulations presented here were performed using the OU Supercomputing Center for Education & Research (OSCER) at the University of Oklahoma (OU).

Furthermore, we would like to thank the anonymous referee for useful suggestions, allowing us to improve the manuscript.

REFERENCES

Airapetian VS, Glocer A, Khazanov GV, Loyd ROP, France K, Sojka J, Danchi WC and Liemohn MW (2017) How hospitable are space weather affected habitable zones? the role of ion escape. *Astrophysical Journal Letters* **836**, L3.

Armstrong DJ, Osborn HP, Brown DJA, Faedi F, Gómez Maqueo Chew Y, Martin DV, Pollacco D and Udry S (2014) On the abundance of circumbinary planets. *Monthly Notices of the Royal Astronomical Society* **444**, 1873.

Baraffe I, Chabrier G, Allard F and Hauschildt PH (1998) Evolutionary models for solar metallicity low-mass stars: mass-magnitude relationships and color-magnitude diagrams. *Astronomy and Astrophysics* **337**, 403.

Chambers JE, Quintana EV, Duncan MJ and Lissauer JJ (2002) Symplectic Integrator Algorithms for Modeling Planetary Accretion in Binary Star Systems. *Astronomical Journal* **123**, 2884.

Cuntz M (2014) *S*-type and *P*-type habitability in stellar binary systems: a comprehensive approach. I. Method and applications. *Astrophysical Journal* **780**, 14.

Cuntz M (2015) *S*-type and *P*-type habitability in stellar binary systems: a comprehensive approach. II. Elliptical orbits. *Astrophysical Journal* **798**, 101.

Cuntz M and Guinan EF (2016) About exobiology: the case for dwarf K stars. *Astrophysical Journal* **827**, 79.

Doyle LR, Carter JA, Fabrycky DC, Slawson RW, Howell SB, Winn JN, Orosz JA, Prša A, Welsh WF, Quinn SN, Latham D, Torres G, Buchhave LA, Marcy GW, Fortney JJ, Shporer A, Ford EB, Lissauer JJ, Ragozzine D, Rucker M, Batalha N, Jenkins JM, Borucki WJ, Koch D, Middour CK, Hall JR, McCauliff S, Fanelli MN, Quintana EV, Holman MJ, Caldwell DA, Still M, Stefanik RP, Brown WR, Esquerdo GA, Tang S, Furesz G, Geary JC, Berlind P, Calkins ML, Short DR, Steffen JH, Sasselov D, Dunham EW, Cochran WD, Boss Alan, Haas MR, Buzasi D and Fischer D (2011) Kepler-16: A Transiting Circumbinary Planet. *Science* **333**, 1602.

Dvorak R (1982) Planetary orbits in double star systems. **Österreichische Akademie der Wissenschaften Mathematisch-Naturwissenschaftliche Sitzungsberichte 191**, 423.

Eggl S., Haghighipour N and Pilat-Lohinger E (2013) Detectability of Earth-like planets in circumstellar habitable zones of binary star systems with Sun-like components. *Astrophysical Journal* **764**, 130.

Grazier KR, Newman WI, Varadi F, Goldstein DJ and Kaula WM (1996) Integrators for long-term solar system dynamical simulations. *Bulletin of the American Astronomical Society* **28**, 1181.

Haghighipour N and Kaltenegger L (2013) Calculating the habitable zone of binary star systems. II. P-type binaries. *Astrophysical Journal* **777**, 166.

Halevy I, Pierrehumbert RT and Schrag DP (2009) Radiative transfer in CO_2-rich paleoatmospheres. *Journal of Geophysical Research* **114**, D18112.

Holman MJ and Wiegert PA (1999) Long-term stability of planets in binary systems. *Astronomical Journal* **117**, 621.

Jones BW, Sleep PN and Chambers JE (2001) The stability of the orbits of terrestrial planets in the habitable zones of known exoplanetary systems. *Astronomy and Astrophysics* **366**, 254.

Kaltenegger L (2017) How to characterize habitable worlds and signs of life. *Annual Review of Astronomy and Astrophysics* **55**, 433.

Kane SR and Hinkel NR (2013) On the habitable zones of circumbinary planetary systems. *Astrophysical Journal* **762**, 7.

Kasting JF, Whitmore DP and Reynolds RT (1993) Habitable zones around main sequence stars. *Icarus* **101**, 108.

Kasting JF, Kopparapu R, Ramirez RM and Harman CE (2014) Remote life-detection criteria, habitable zone boundaries, and the frequency of Earth-like planets around M and late K stars. *Proceedings of the National Academy of Sciences* **111**, 12641.

Kirk B, Conroy K, Prša A, Abdul-Masih M, Kochoska A, Matijevič G, Hambleton K, Barclay T, Bloemen S, Boyajian T, Doyle LR, Fulton BJ, Hoekstra AJ, Jek K, Kane SR, Kostov V, Latham D, Mazeh T, Orosz JA, Pepper J, Quarles B, Ragozzine D, Shporer A, Southworth J, Stassun K, Thompson SE, Welsh WF, Agol E, Derekas A, Devor J, Fischer D, Green G, Gropp J, Jacobs T, Johnston C, LaCourse DM, Saetre K, Schwengeler H, Toczyski J, Werner G, Garrett M, Gore J, Martinez AO, Spitzer I, Stevick

J, Thomadis PC, Vrijmoet EH, Yenawine M, Batalha N and Borucki W (2016) Kepler eclipsing binary stars. VII. The catalog of eclipsing binaries found in the entire Kepler data set. *Astronomical Journal* **151**, 68.

Kirkpatrick JD, Henry TJ and McCarthy DW Jr (1991) A standard stellar spectral sequence in the red/near-infrared — classes K5 to M9. *Astrophysical Journal Supplement Series* **77**, 417.

Kitzmann D (2016) Revisiting the scattering greenhouse effect of CO_2 ice clouds. *Astrophysical Journal Letters* **817**, L18.

Kopparapu RK, Ramirez R, Kasting JF, Eymet V, Robinson TD, Mahadevan S, Terrien RC, Domagal-Goldman S, Meadows V and Deshpande R (2013) Habitable zones around main-sequence stars: new estimates. *Astrophysical Journal* **765**, 131; Erratum **770**, 82.

Kopparapu RK, Ramirez RM, SchottelKotte J., Kasting JF, Domagal-Goldman S and Eymet V (2014) Habitable zones around main-sequence stars: dependence on planetary mass *Astrophysical Journal* **787**, L29.

Kostov VB, Orosz JA, Welsh WF, Doyle LR, Fabrycky DC, Haghighipour N, Quarles B, Short DR, Cochran WD, Endl M, Ford EB, Gregorio J, Hinse TC, Isaacson H, Jenkins JM, Jensen ELN, Kane S, Kull I, Latham DW, Lissauer JJ, Marcy GW, Mazeh T, Müller TWA, Pepper J, Quinn SN, Ragozzine D, Shporer A, Steffen JH, Torres G, Windmiller G and Borucki WJ (2016) Kepler-1647b: the largest and longest-period Kepler transiting circumbinary planet. *Astrophysical Journal* **827**, 86.

Lammer H (2007) M star planet habitability. *Astrobiology* **7**, 27.

Lammer H, Bredehöft JH, Coustenis A, Coustenis A, Khodachenko ML, Kaltenegger L, Grasset O, Prieur D, Raulin F, Ehrenfreund P, Yamauchi M, Wahlund J-E, Grießmeier J-M, Stangl G, Cockell CS, Kulikov YuN, Grenfell JL and Rauer H (2009) What makes a planet habitable? *Astronomy and Astrophysics Reviews* **17**, 181.

Mann AW, Gaidos E and Ansdell M (2013) Spectro-thermometry of M dwarfs and their candidate planets: too hot, too cool, or just right? *Astrophysical Journal* **779**, 188.

Mischna MA, Kasting JF, Pavlov A and Freedman R (2000) Influence of carbon dioxide clouds on early martian climate. *Icarus* **145**, 546.

Pierrehumbert R and Gaidos E (2011) Hydrogen greenhouse planets beyond the habitable zone. *Astrophysical Journal Letters* **734**, L13.

Popp M and Eggl S (2017) 3D climate simulations of an Earth-like circumbinary planet. *19th European Geosciences Union General Assembly* **EGU2017**, 9885.

Press WH, Flannery BP, Teukolsky SA and Vetterling WT (1986) *Numerical Recipes: The Art of Scientific Computing* (Cambridge: Cambridge Univ. Press).

Quarles B, Musielak ZE and Cuntz M (2012) Habitability of Earth-mass planets and moons in the Kepler-16 system. *Astrophysical Journal* **750**, 14 (QMC12).

Raghavan D, Henry TJ, Mason BD, Subasavage JP, Jao W-C, Beaulieu TD and Hambly NC (2006) Two Suns in the sky: stellar multiplicity in exoplanet systems. *Astrophysical Journal* **646**, 523.

Raghavan D, McAlister HA, Henry TJ, Latham DW, Marcy GW, Mason BD, Gies DR, White RJ and ten Brummelaar TA (2010) A survey of stellar families: multiplicity of solar-type stars. *Astrophysical Journal Supplement Series* **190**, 1.

Roell T, Neuhäuser R, Seifahrt A and Mugrauer M (2012) Extrasolar planets in stellar multiple systems. *Astronomy and Astrophysics* **542**, A92.

Seager S (2013) Exoplanet habitability. *Science* **340**, 577.

Selsis F, Kasting JF, Levrard B, Paillet J, Ribas I and Delfosse X (2007) Habitable planets around the star Gliese 581? *Astronomy and Astrophysics* **476**, 1373.

Shevchenko II (2017) Habitability properties of circumbinary planets. *Astronomical Journal* **153**, 273.

Slawson RW, Prša A, Welsh WF, Orosz JA, Rucker M, Batalha N, Doyle LR, Engle SG, Conroy K, Coughlin J, Gregg TA, Fetherolf T, Short DR, Windmiller G, Fabrycky DC, Howell SB, Jenkins JM, Uddin K, Mullally F, Seader SE, Thompson SE, Sanderfer DT, Borucki W and Koch D (2011) Kepler eclipsing binary stars. II. 2165 eclipsing binaries in the second data release. *Astronomical Journal* **142**, 160.

Tarter JC, Backus PR, Mancinelli RL, Aurnou JM, Backman DE, Basri GS, Boss AP, Clarke A, Deming D, Doyle LR, Feigelson ED, Freund F, Grinspoon DH, Haberle RM, Hauck SA II, Heath MJ, Henry TJ, Hollingsworth JL, Joshi MM, Kilston S, Liu MC, Meikle E, Reid IN, Rothschild LJ, Scalo J,

Segura A, Tang CM, Tiedje JM, Turnbull MC, Walkowicz LM, Weber AL and Young RE (2007) A reappraisal of the habitability of planets around M dwarf stars. *Astrobiology* **7**, 30.

Thompson SE, Coughlin JL, Hoffman K, Mullally F, Christiansen JL, Burke CJ, Bryson S, Batalha N, Haas MR, Catanzarite J, Rowe JF, Barentsen G, Caldwell DA, Clarke BD, Jenkins JM, Li J, Latham DW, Lissauer JJ, Mathur S, Morris RL, Seader SE, Smith JC, Klaus TC, Twicken JD, Wohler B, Akeson R, Ciardi DR, Cochran WD, Barclay T, Campbell JR, Chaplin WJ, Charbonneau D, Henze CE, Howell SB, Huber D, Prsa A, Ramirez SV, Morton TD, Christensen-Dalsgaard J, Dotson JL, Doyle L, Dunham EW, Dupree AK, Ford EB, Geary JC, Girouard FR, Isaacson H, Kjeldsen H, Steffen JH, Quintana EV, Ragozzine D, Shporer A, Silva Aguirre V, Still M, Tenenbaum P, Welsh WF, Wolfgang A, Zamudio KA, Koch DG and Borucki WJ (2017) Planetary candidates observed by Kepler. VIII. A fully automated catalog with measured completeness and reliability based on data release 25. *Astrophysical Journal Supplement Series* submitted; arXiv:1710.06758.

Underwood DR, Jones BW and Sleep PN (2003) The evolution of habitable zones during stellar lifetimes and its implications on the search for extraterrestrial life. *International Journal of Astrobiology* **2**, 289.

von Bloh W, Bounama C, Cuntz M and Franck S (2007) The habitability of super-Earths in Gliese 581. *Astronomy and Astrophysics* **476**, 1365.

Wang J, Fischer DA, Xie J-W and Ciardi DR (2014) Influence of stellar multiplicity on planet formation. II. Planets are less common in multiple-star systems with separations smaller than 1500 AU. *Astrophysical Journal* **791**, 111.

Wang, Zh and Cuntz M (2017) Fitting formulae and constraints for the existence of S-type and P-type habitable zones in binary systems. *Astronomical Journal* **154**, 157.

Welsh WF, Orosz JA, Short DR, Cochran WD, Endl M, Brugamyer E, Haghighipour N, Buchhave LA, Doyle LR, Fabrycky DC, Hinse TC, Kane SR, Kostov V, Mazeh T, Mills SM, Müller TWA, Quarles B, Quinn SN, Ragozzine D, Shporer Avi, Steffen JH, Tal-Or L, Torres G, Windmiller G and Borucki WJ (2015) Kepler 453b — the 10th Kepler transiting circumbinary planet. *Astrophysical Journal* **809**, 26.

Williams DM and Pollard D (2002) Earth-like worlds on eccentric orbits: excursions beyond the habitable zone. *International Journal of Astrobiology* **1**, 61.

Wordsworth R, Forget F, Millour E, Head JW, Madeleine J-B and Charnay B (2013) Global modelling of the early martian climate under a denser CO_2 atmosphere: water cycle and ice evolution. *Icarus* **222**, 1.

Zuluaga JI, Mason PA and Cuartas-Restrepo PA (2016) Constraining the radiation and plasma environment of the Kepler circumbinary habitable-zone planets. *Astrophysical Journal* **818**, 160.

This preprint was prepared with the AAS LaTeX macros v5.0.

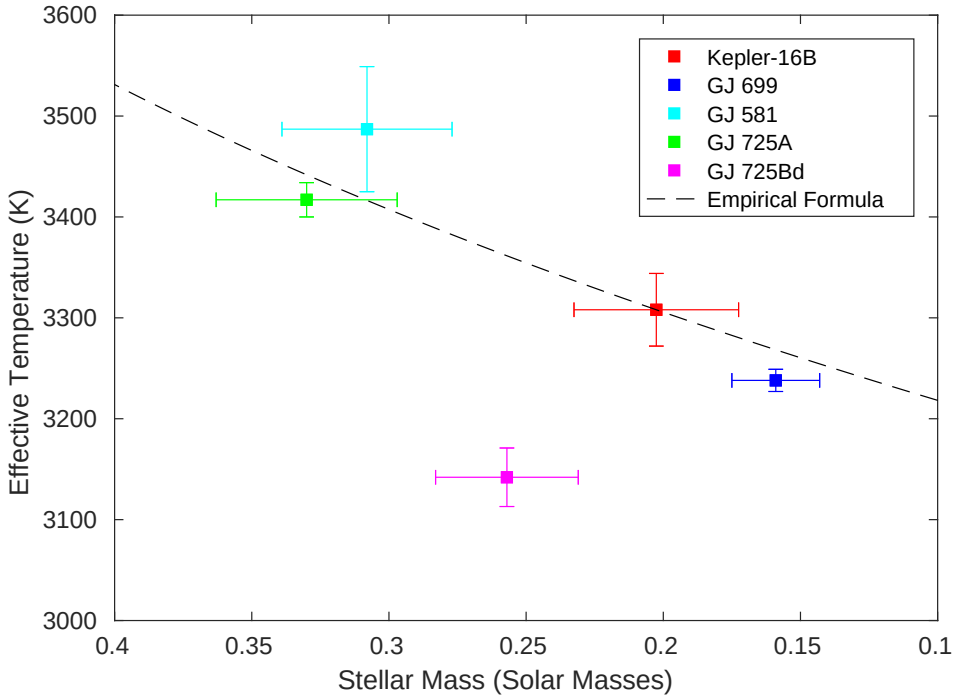


Fig. 1.—: Depiction of the effective temperature of Kepler-16B determined via an empirical formula given by Mann *et al.* (2013) that relates the mass to the effective temperature, and vice versa, for M dwarf stars. By knowing the mass of Kepler-16B, its effective temperature can be extracted, resulting in an effective temperature of 3308 ± 110 K. In addition, a subset of the sample of M dwarf stars is depicted, used to derive the adopted empirical formula.

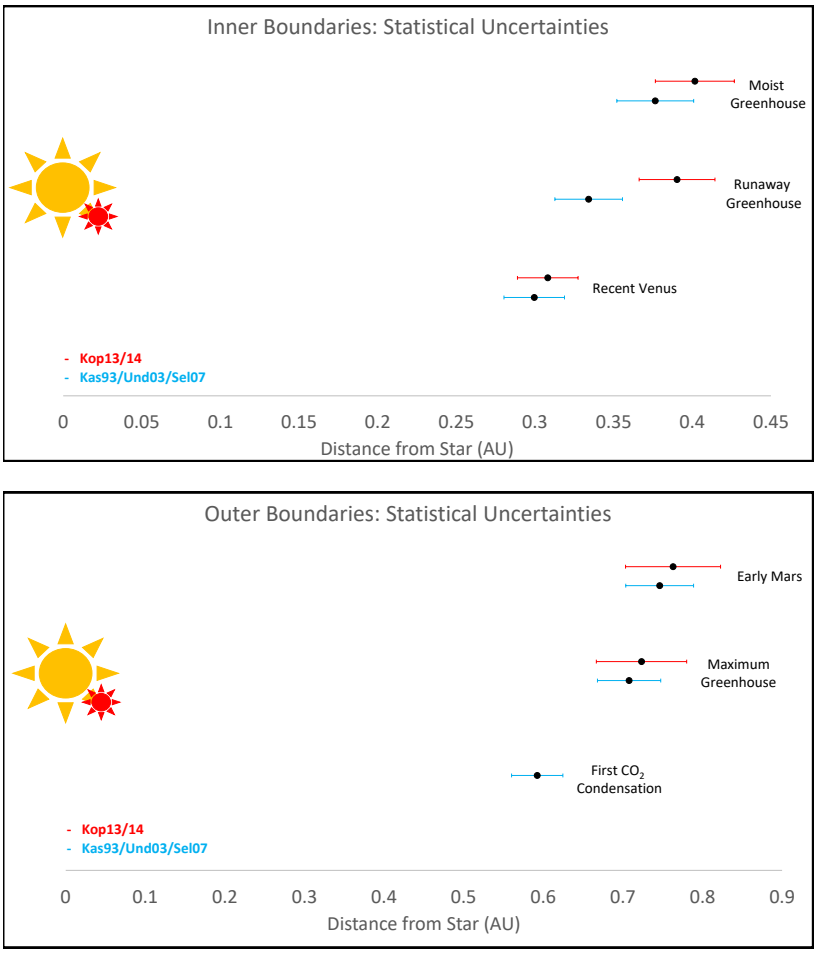


Fig. 2.—: Inner and outer HZ limits for Kepler-16A (single star approach) while comparing two different determination methods. We also include information on the inherent statistical uncertainties of those based on Press *et al.* (1986) (see also Table 3). The blue data correspond to the inner and outer HZ boundaries as expected from utilizing the method of Kasting *et al.* (1993) with updates by Underwood *et al.* (2003) and Selsis *et al.* (2007). Conversely, the red data correspond to the inner and outer HZ limits as expected from utilizing the method specified by Kopparapu *et al.* (2013, 2014).

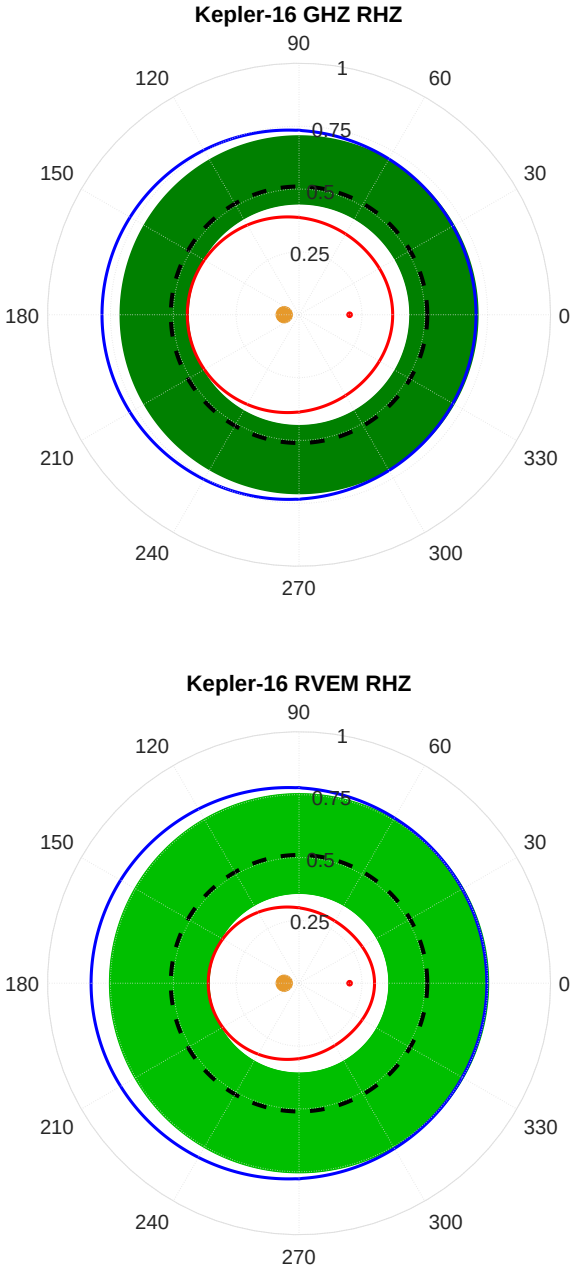


Fig. 3.—: Depiction of the RHZ for the GHZ and RVEM criteria based on methods given by Cuntz (2014, 2015) and Wang & Cuntz (2017). In both plots the red and blue lines correspond to the inner and outer RHZ limits with the inner HZ limit defined as the maximum radial distance of the inner RHZ (red lines) and the outer HZ limit defined as the minimum radial distance of the outer RHZ (blue lines). This approach produces the conventional HZ region for GHZ (darkest green) and RVEM (medium green) criteria. As expected the RVEM criteria produces a more generous HZ region as shown. Lastly, the black dashed line represents the orbital stability limit, calculated using the formula provided by Holman & Wiegert (1999) for P-type orbits, in which bodies exterior to that line are orbitally stable while bodies interior to that line are orbitally unstable.

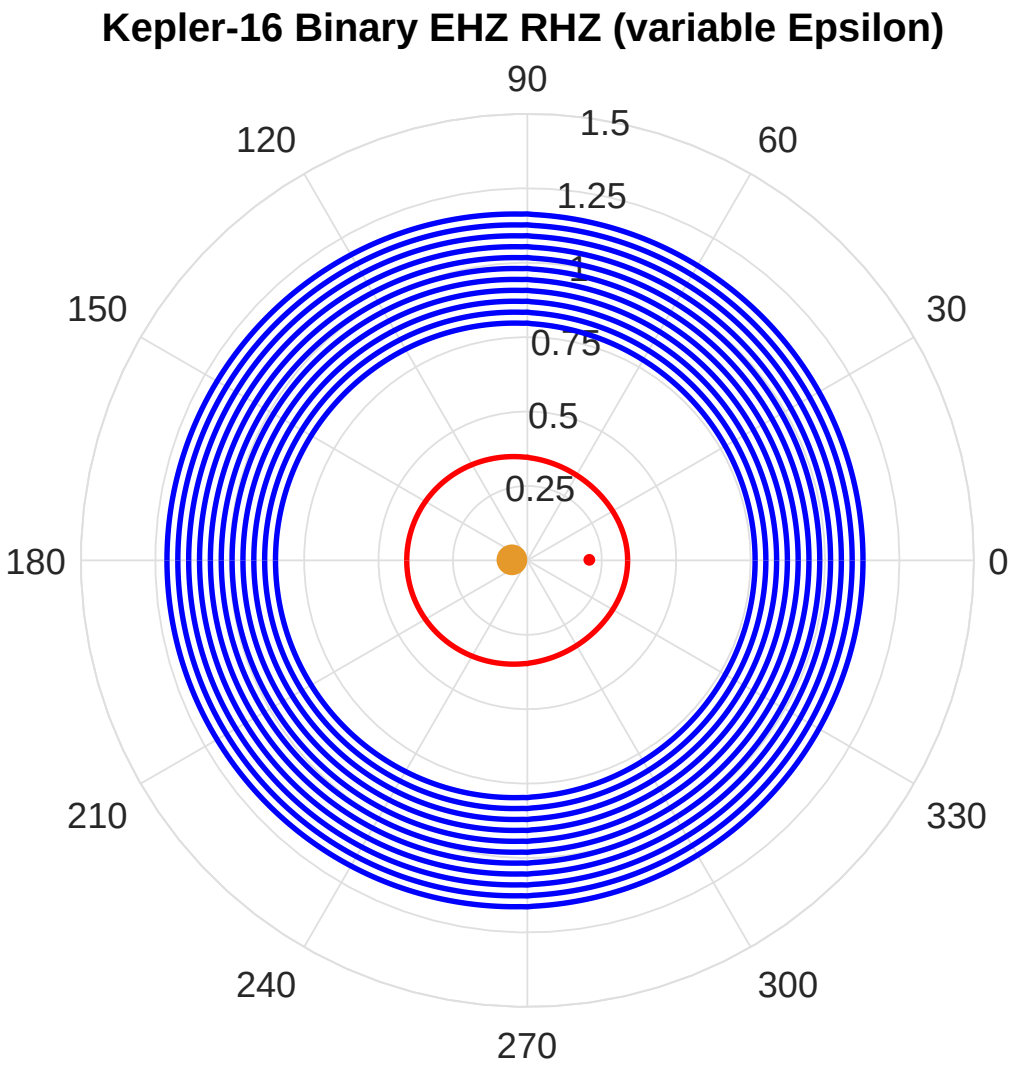


Fig. 4.—: Different outer boundaries (blue lines) of the EHZ resulting from the different epsilon values ranging from $\epsilon = 2.0$ (innermost blue line) to $\epsilon = 3.0$ (outermost blue line). A median value of $\epsilon = 2.5$ has been chosen for our definition of the EHZ akin to Mischna *et al.* (2000), which is also adopted for our analysis in the subsequent Figs. 7, 8, and 10 and depicted as the lightest green regions.

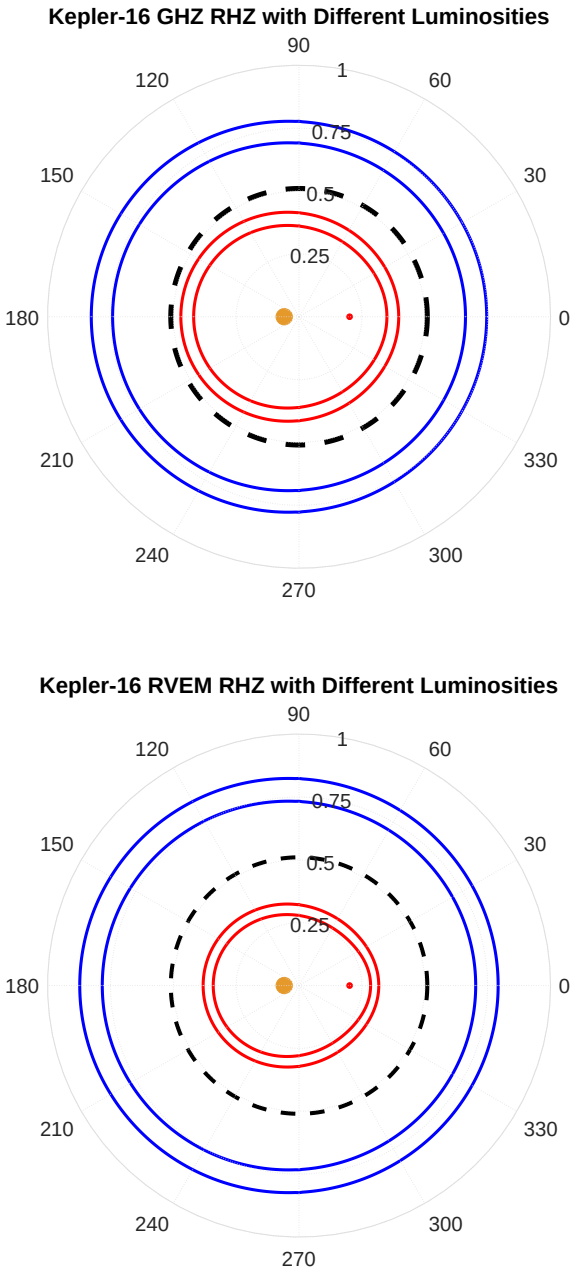


Fig. 5.—: Depiction of the inner and outer boundaries of the GHZ and RVEM, while utilizing the upper and lower bounds of the stellar luminosities to illustrate how the uncertainty in the luminosity affects the determination of the HZs. In both plots the inner and outer HZ limits are shown in red and blue, respectively, with the inner sets of red and blue lines corresponding to the lower bound luminosity and the outer sets of red and blue lines corresponding to the upper bound luminosity. As expected, the upper bound luminosity shifts the GHZ and RVEM limits outward while the lower bound luminosity shifts those limits inward.

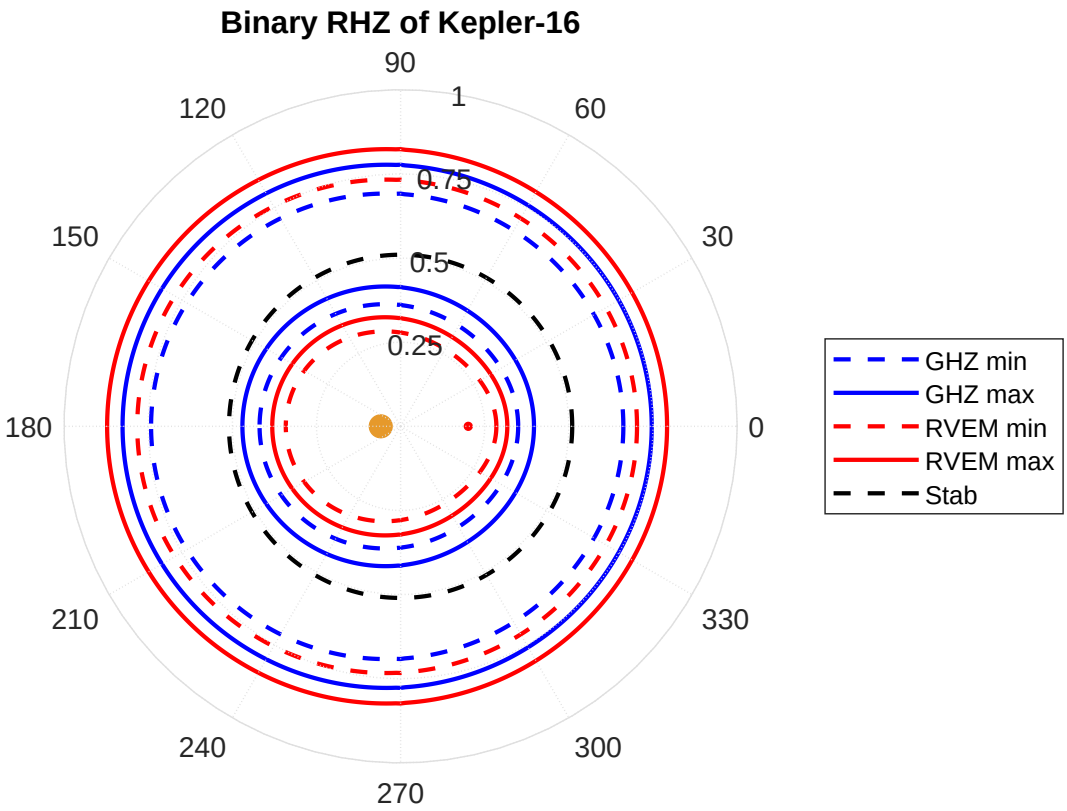


Fig. 6.—: Similar to Fig. 5, as this figure combines the inner and outer boundaries for the GHZ and RVEM criteria while also incorporating the upper and lower luminosity bounds; its emphasis is to illustrate the extents of the achievable HZs based on luminosity and HZ criteria specification. Additionally, the black dashed line represents the orbital stability limit. The blue and red dotted lines correspond to the minimum possible inner limits (associated with the lower bound luminosity) for the GHZ and RVEM, respectively. The blue and red solid lines correspond to the maximum possible outer limits (associated with the upper bound luminosity) for GHZ and RVEM, respectively.

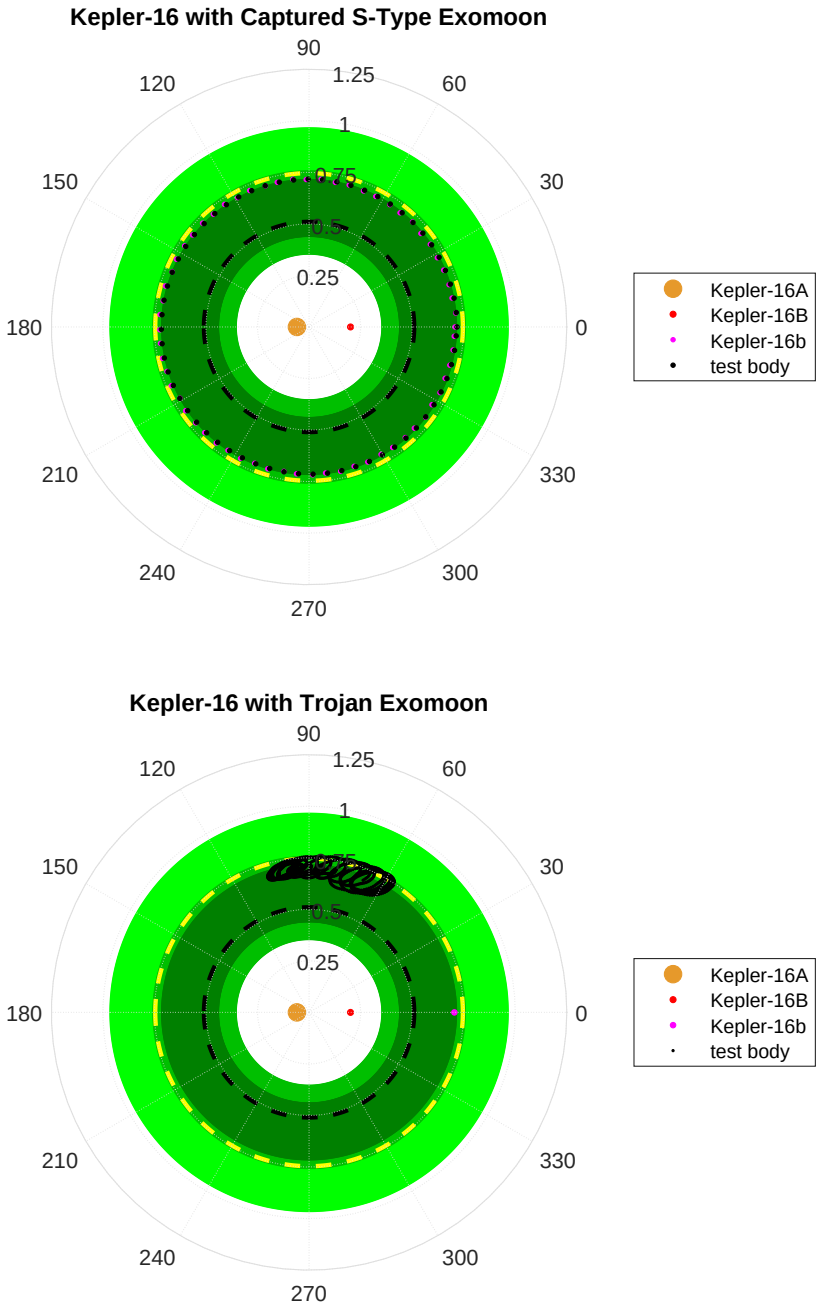


Fig. 7.—: Illustration of previous results by QMC12 with updated HZ regions. (a) Depiction of an S-type captured Earth-mass exomoon (black in QMC12); the primary and secondary stars (orange and red in QMC12, respectively) and the Saturnian planet Kepler-16b are also given (magenta in QMC12). (b) Depiction of a possible Trojan exomoon in a rotating reference frame (black in QMC12). The darkest green region represents the GHZ, the medium green region represents the RVEM, and the lightest green region represents the EHZ. The dashed yellow line represents the outer limit of the GHZ if the stellar luminosities are assumed at their upper limits as informed by the observational uncertainties.

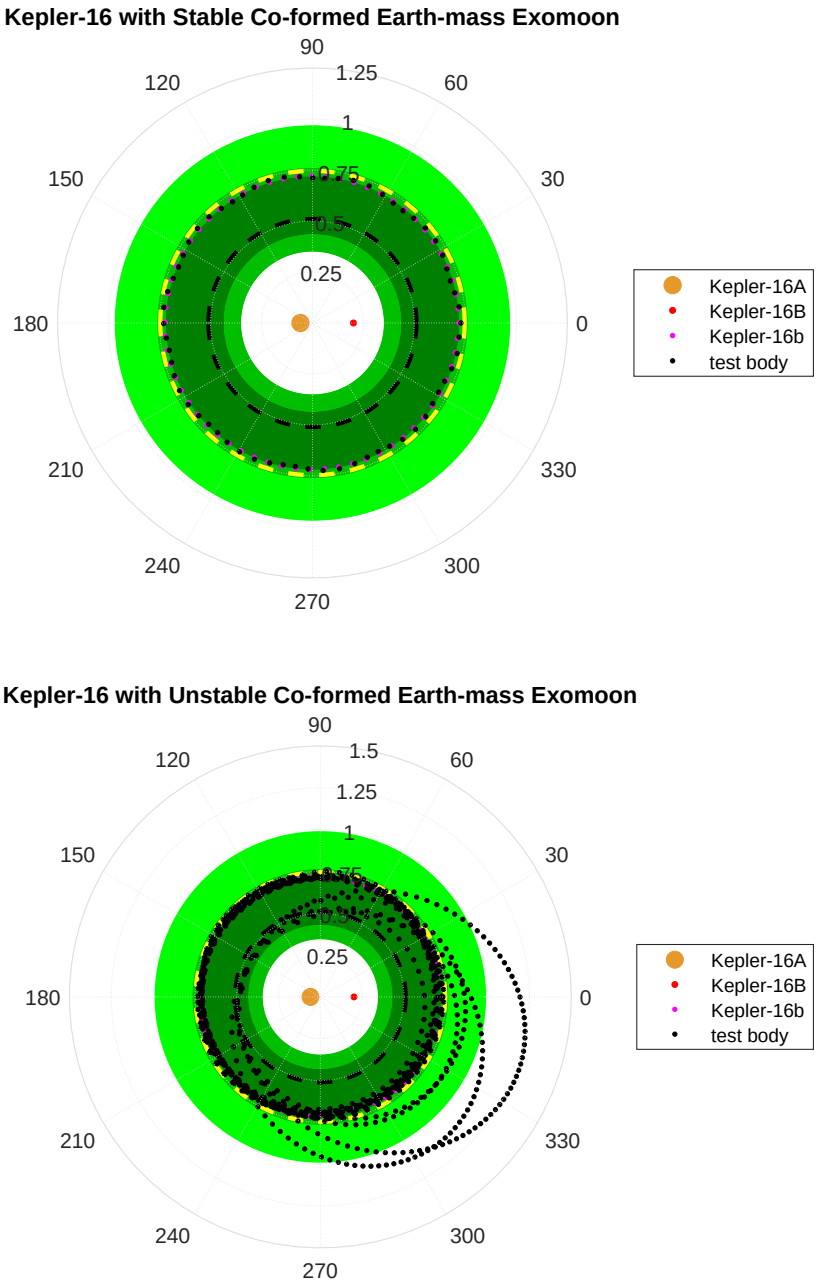


Fig. 8.—: Illustration of the previous results by QMC12 with updated HZ regions. (a) Depiction of a stable S-type coformed Earth-mass exomoon (black in QMC12); the primary and secondary stars (orange and red in QMC12, respectively) and the Saturnian planet Kepler-16b are also given (magenta in QMC12). (b) Depiction of an unstable S-type coformed Earth-mass exomoon (black in QMC12). See Fig. 7 for information on the color coding of the HZs.

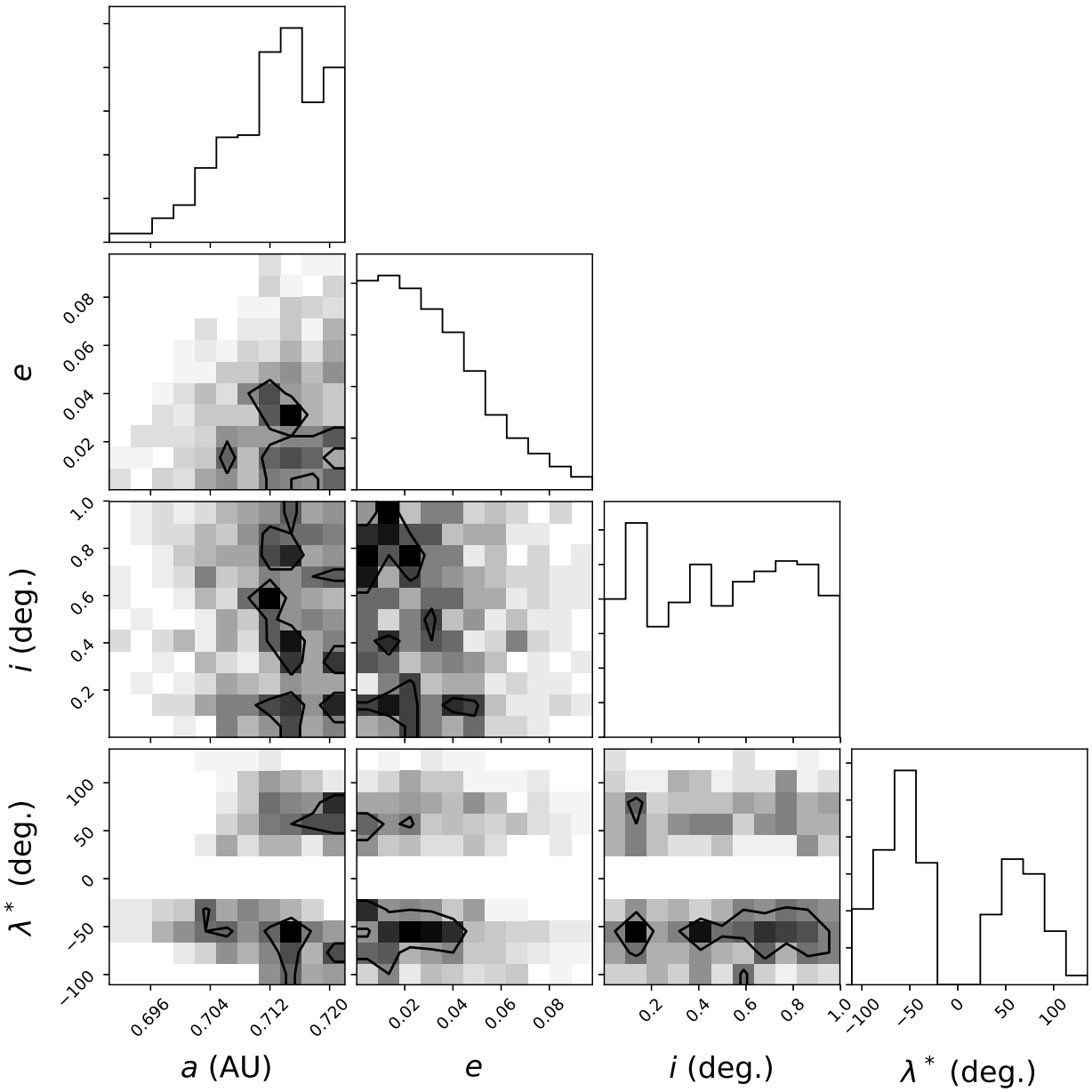


Fig. 9.—: Distributions of the initial semimajor axis a, eccentricity e, inclination i, and relative mean longitude λ^*, given as $\lambda^* = \lambda_\oplus - \lambda_{16\mathrm{B}}$ that produces a stable Earth-mass co-orbital planet in Kepler-16. These initial conditions are chosen relative to the center-of-mass of the stellar components.

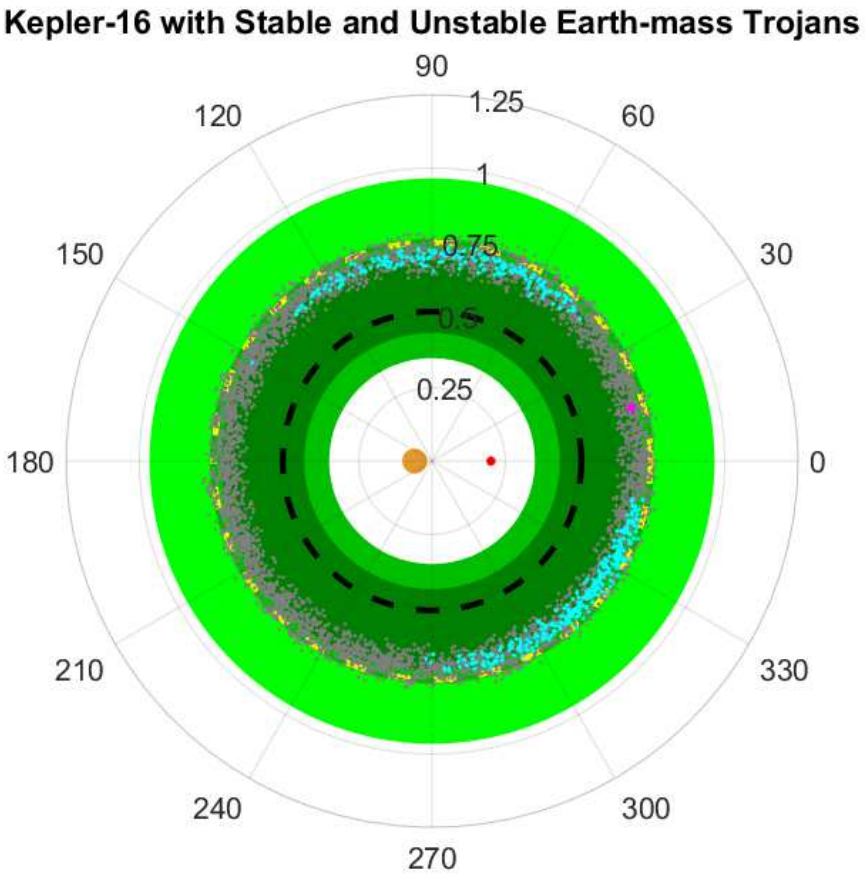


Fig. 10.—: Illustration of the starting locations of stable (cyan) and unstable (gray) initial conditions out of 5,000 trials. These simulations differ from QMC12 as the relative phase between the binary and planetary orbit is now taken into account, where the positive x-axis is taken to be the line-of-sight. See Fig. 7 for information on the color coding of the HZs.

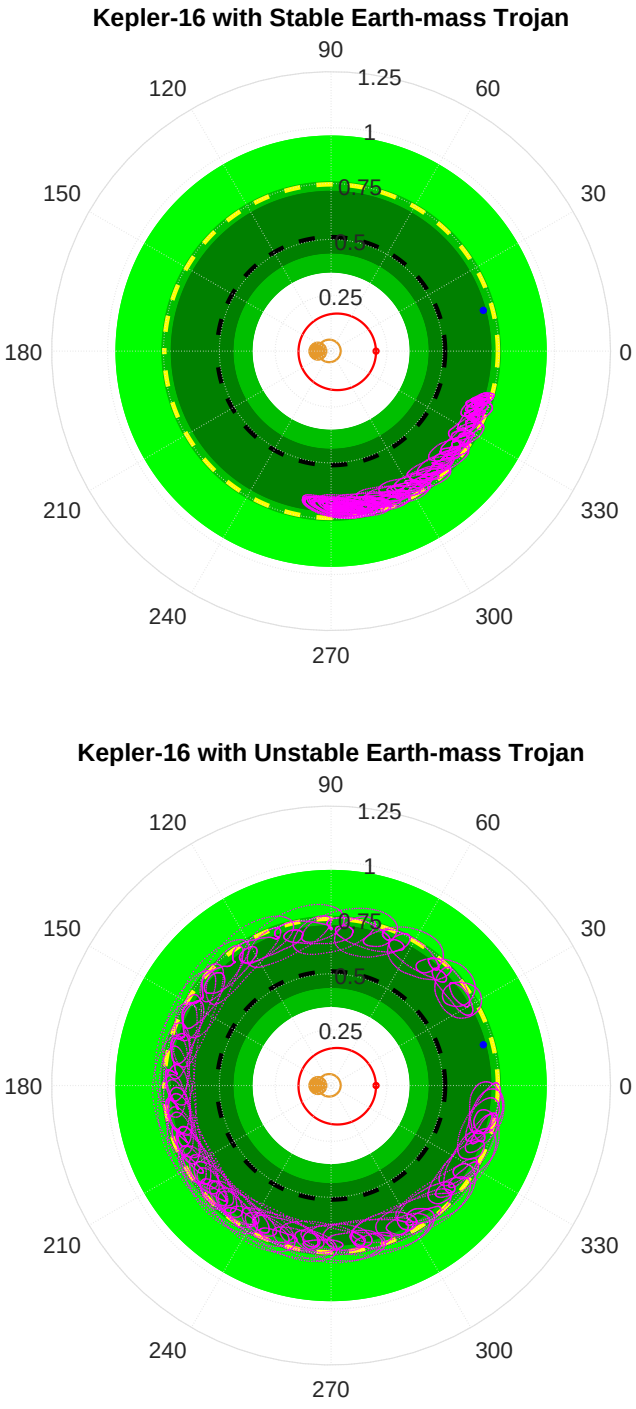


Fig. 11.—: Examples of orbital evolution (magenta) of a stable (top) and unstable (bottom) Earth-mass planet co-orbiting with Kepler-16b. These orbits are shown in a rotated-reference frame depicting the relative motions with Kepler-16b to illustrate Trojan (top) and horseshoe (bottom) configurations. See Fig. 7 for information on the color coding of the HZs.

Table 1. Stellar and Planetary Parameters of Kepler-16

Parameter	Value[a]
Distance (pc)	~ 61
$F_{\rm B}/F_{\rm A}$	0.01555 ± 0.0001
M_1 ($M_\odot$)	0.6897 ± 0.0035
M_2 ($M_\odot$)	0.20255 ± 0.00066
$T_{\rm eff,1}$ (K)	4450 ± 150
$T_{\rm eff,2}$ (K)	3308 ± 110
R_1 ($R_\odot$)	0.6489 ± 0.0013
R_2 ($R_\odot$)	0.22623 ± 0.00059
$P_{\rm b}$ (d)	41.079220 ± 0.000078
$a_{\rm b}$ (AU)	0.22431 ± 0.00035
$e_{\rm b}$	0.15944 ± 0.00061
$M_{\rm p}$ ($M_{\rm J}$)	0.333 ± 0.016
$a_{\rm p}$ (AU)	0.7048 ± 0.0011
$e_{\rm p}$	0.0069 ± 0.001

Note. — [a]Data as provided by Doyle *et al.* (2011) and reported by QMC12, except for $T_{\rm eff,2}$ and R_2, which have been determined in this study. All parameters have their usual meaning.

Table 2. Percentage Uncertainty of Kepler-16 Parameters

Parameter	% Uncertainty
F_B/F_A	0.64
M_1 ($M_\odot$)	0.51
M_2 ($M_\odot$)	0.33
$T_{\rm eff,1}$ (K)	3.37
$T_{\rm eff,2}$ (K)	3.33
R_1 ($R_\odot$)	0.20
R_2 ($R_\odot$)	0.26

Table 3. Single Star Habitable Zone Limits

Habitable Zone Limit	Kas93/Und03	Kop1314	HZ Type
Recent Venus	0.299	0.308	RVEM (in)
Runaway Greenhouse	0.334	0.390	GHZ (in)
Water Loss	0.376	0.402	...
First CO_2 Condensation	0.592	...	...
Maximum Greenhouse	0.708	0.723	GHZ (out)
Early Mars	0.746	0.766	RVEM (out)

Note. — Kas93: Kasting *et al.* (1993), Und03: Underwood *et al.* (2003), Kop1314: Kopparapu *et al.* (2013, 2014)

Table 4. Statistical Uncertainties

Habitable Zone Limit	Kas93/Und03		Kop1314	
...	Min-Max	Statis	Min-Max	Statis
Recent Venus	1.97 %	1.93 %	1.98 %	1.93 %
Runaway Greenhouse	2.21 %	2.15 %	2.51 %	2.41 %
Water Loss	2.51 %	2.44 %	2.59 %	2.51 %
First CO_2 Condensation	3.34 %	3.22 %	...	...
Maximum Greenhouse	4.14 %	3.98 %	4.15 %	5.67 %
Early Mars	4.40 %	4.26 %	4.39 %	5.97 %

Note. — For references, see comments of Table 3. Min-Max means that the minimum/maximum values for the luminosities and effective temperatures are applied. Statis means adequately applied statistical uncertainty propagation.

Table 5. GHZ and RVEM RHZs of Binary System

Reference Distance ...	GHZ (AU)	RVEM (AU)	Relevance ...
Inner RHZ Limit, innermost	0.368	0.285	No
Inner RHZ Limit, outermost	0.444	0.361	Yes
Outer RHZ Limit, innermost	0.704	0.747	Yes
Outer RHZ Limit, outermost	0.783	0.827	No
Orbital Stability Limit	0.510	0.510	Yes

Note. — The RHZ bounds have previously been referred to as RHLs (Cuntz 2014). Here the innermost and outermost points of these limits are reported, which are of different relevance for setting the respective RHZ.

Table 6. EHZ of Kepler-16(AB)

ϵ ...	EHZ (AU)
2.0	0.765
2.1	0.801
2.2	0.837
2.3	0.873
2.4	0.910
2.5	0.946
2.6	0.982
2.7	1.018
2.8	1.055
2.9	1.091
3.0	1.127

Table 7. Comparison of Habitable Zone Limits

Type	Single Star		Binary System Approach					
...	GHZ	RVEM	GHZ	GHZ (L^-)	GHZ (L^+)	RVEM	RVEM (L^-)	RVEM (L^+)
...	(AU)	(AU)	(AU)	(AU)	(AU)	(AU)	(AU)	(AU)
$\mathrm{RHZ_{in}}$	0.390	0.308	0.444	0.419	0.470	0.361	0.341	0.381
$\mathrm{RHZ_{out}}$	0.723	0.763	0.704	0.662	0.746	0.747	0.702	0.792
a_{orb}	...	...	0.510	0.510	0.510	0.510	0.510	0.510
ΔHZ	0.333	0.455	0.194	0.152	0.236	0.237	0.192	0.282
Type	...	...	PT	PT	PT	PT	PT	PT

Note. — L^+ and L^- indicate $L \pm \Delta L$, respectively, with variations in T_{eff} and R simultaneously applied to both stellar components (see Table 1). ΔHZ indicates the width of the HZ with consideration of the orbital stability limit, if applicable. PT conveys that the P-type HZ is truncated due to the additional requirement of orbital stability.

Table 8. Initial Conditions for Exomoon Sample Cases

Publication	Type	a (AU)	e	i (°)	ω (°)	M (°)
QMC12	Kepler-16(AB)	0.22431	0.15944	0	0	180
	Kepler-16(AB)b	0.7048	0.0069	0	180	180
	Stable Retrograde	0.619	0.13	180	180	180
	Stable Trojan	0.7048	0.0069	0	180	240
	Stable Prograde	0.715	0	0	180	180
	Unstable Prograde	0.721	0	0	180	180
This Work	Kepler-16(AB)	0.22431	0.15944	0	263.464	−171.114
	Kepler-16(AB)b	0.7048	0.0069	0.3079	318	−211.49
	Stable Trojan	0.7096	0.0088	0.8175	37.499	35.272
	Unstable Trojan	0.6902	0.0651	0.0795	124.235	154.849

Note. — Initial conditions in terms of orbital elements for the binary (Kepler-16(AB)), the Saturnian planet (Kepler-16b), and the possible Earth-mass exomoon. These orbital elements can be used to reproduce our new results (Fig. 11) and the previous results of QMC12 (Figs. 7 and 8).